Semiconductor Physics, Quantum Electronics & Optoelectronics, 2015. V. 18, N 1. P. 12-19.
doi: 10.15407/ spqeo18.01.012

PACS 71.15.-m, 71.20.-b

Electronic structure of $PbSnS_3$ and $PbGeS_3$ semiconductor compounds with the mixed cation coordination

M.M. Bletskan[1], D.I. Bletskan[1], V.M. Kabatsii[21]
[1]*Uzhgorod National University, 54, Voloshin str., 88000 Uzhgorod, Ukraine*
[2]*Mukachevo State University, 26, Uzhgorodska str., 89600 Mukachevo, Ukraine*
E-mail: crystal_lab457@yahoo.com

Abstract. The self-consistent band structure calculation of $PbSnS_3$ and $PbGeS_3$ ternary compounds with the mixed cation coordination was performed using the *ab initio* density functional theory method. It has been found that both compounds are indirect-gap semiconductors. The calculated band-gap widths are E_{gi} = 0.75 eV for $PbSnS_3$ and E_{gi} = 1.96 eV for $PbGeS_3$. It was performed the analysis of partial contributions to the total density of electronic states, which allowed to identify the genetic nature of valence and conduction bands. The feature of the structure of occupied energy bands in these compounds is the presence of isolated quasi-core *d*-band of lead atoms and the contribution of Pb6*s*-states of lone-electron pair to the top of valence band as well as to the second occupied subband. The electron density maps in the different planes have been analyzed. They clearly demonstrate presence of covalent-ionic bond character within the infinite chains and ribbons with prevailing charge concentration on Ge–S, Sn–S, Pb–S bonds, and a weak van der Waals bond component with participation of lone-electron pair of lead between layers as well as ribbons.

Keywords: suredaite, lead thiogermanate, mixed valence, electronic structure, density of states, lone-electron pair.

Manuscript received 13.10.14; revised version received 17.12.14; accepted for publication 19.02.15; published online 26.02.15.

1. Introduction

Interaction of group IV elements (Ge, Sn, Pb) with chalcogens (S, Se) depending on a component ratio leads to formation of binary compounds where cations exhibit different valences (II or IV) [1]. Thus, the cations in germanium and tin monochalcogenides, crystallized in orthorhombic structure, have the valence II (M^{II} = Ge^{2+}, Sn^{2+}). The cations in germanium and tin dichalcogenides have the valence IV (M^{IV} = Ge^{4+}, Sn^{4+}). Though the tetravalent states of germanium and tin atoms are the most stable, there are also known ternary chalcogenides with different oxidation states of the group IV atoms. So, the interaction of $M^{II}X$ and $M^{IV}X_2$ binary compounds with octahedral and tetrahedral coordinations leads to formation of $M^{II}M^{IV}S_3$ ternary compounds with the mixed cation coordinations [1]. In binary and ternary compounds, in which the group IV elements exhibit the valence II, only their *p*-states are involved in formation of chemical bonds, while *s*-states are not directly involved in chemical bond formation, and they represent lone-electron pairs.

We chose $PbSnS_3$ and $PbGeS_3$ as the objects for electronic structure study of the $M^{II}M^{IV}S_3$-type (where

Semiconductor Physics, Quantum Electronics & Optoelectronics, 2015. V. 18, N 1. P. 12-19.
doi: 10.15407/ spqeo18.01.012

M^{II} = Pb^{II}, Sn^{II}; M^{IV} = Ge^{IV}, Sn^{IV}) compounds with the mixed valence. In the nature, $PbSnS_3$ compound meets as suredaite mineral [2], and it is still poorly studied. In the literature there are only data on the study of electrical conductivity [3, 4] and fundamental absorption edge [3, 5] of $PbSnS_3$ crystals.

The characteristic feature of lead thiogermanate ($PbGeS_3$) is the opportunity to obtain it in crystalline and glassy states [1]. Unlike to $PbSnS_3$, the physical properties of crystalline and glassy $PbGeS_3$ are investigated in more details. Thus, IR and Raman spectra are studied in Refs. [6-8], and the detailed research results of edge absorption [3, 9] and photoconductivity [10] of ordered and disordered phases are given in the wide temperature range.

The electronic structure is one of the fundamental characteristics that substantially defines the main crystal properties. The electronic structure calculations of $PbGeS_3$ crystal were not previously performed. The first results of the studying of $PbSnS_3$ electronic structure are presented in Refs. [11, 12]. These works briefly describe the band structure of $PbSnS_3$, while the discussion of chemical bond nature and the role of lone pair of lead in electronic structure formation are not considered. Therefore, it is very important to ascertain the role of lone-electron pair in band structure formation in the given class of compounds.

In this paper, we present the calculation results of electronic band structure, total and local partial density of electronic states, spatial distribution of valence electronic density of $PbSnS_3$ and $PbGeS_3$ crystals using non-empirical *ab initio* density functional theory (DFT) method in the plane-wave (PW) as well as linear combination of atomic orbitals (LCAO) basis sets with geometry optimization (lattice parameters and atom positions in the unit cell).

2. Crystal structure of $PbSnS_3$ and $PbGeS_3$

The crystal structure of $M^{II}M^{IV}S_3$-type compounds is described by the dense packing of anions, where cations occupy octahedral and tetrahedral voids. The determining factor of structure formation is the tendency of cations to a certain type of coordination depending on its nature, types of anions and species of other sort cations presented in the crystal. The coordination environment of Pb^{2+} cations is tetrahedral in $PbSnS_3$ and octahedral in $PbGeS_3$.

Under laboratory conditions, $PbSnS_3$ compound is obtained by direct fusion of PbS and SnS_2 mixture of the equimolar composition at the temperature 973 K [13]. $PbSnS_3$ compound crystallizes in the orthorhombic structure, which symmetry is described by *Pnma* space group with the lattice parameters a = 8.738 Å, b = 3.792 Å and c = 14.052 Å [13]. The lattice parameters of a natural suredaite mineral slightly differ (a = 8.822 Å, b = 3.773 Å and c = 14.008 Å), which is mainly related with availability of a large amount of impurities in its composition [2].

The number of formula units in the unit cell is Z = 4. The valence of lead in $PbSnS_3$ compound is II and that of tin – IV. The unit cell of $PbSnS_3$ contains twenty atoms, including four Pb^{II}, four Sn^{IV}, and twelve S. Pb^{II} and Sn^{IV} atoms are in non-equivalent positions of crystal lattice. Bivalent Pb^{II}, tetravalent Sn^{IV} and three sulfur S(1), S(2), S(3) atoms occupy five different 4*c* positions of *Pnma* space group. The crystal structure of $PbSnS_3$ is built by deformed $[Sn^{IV}S_6]$ octahedra linked among themselves by common edges in infinite dual chains extended along [010] direction (Fig. 1). The endless ribbons are formed by adjoin of $[Pb^{II}S_3{\bullet}E{\bullet}]$ ψ-tetrahedra on both sides of dual chains.

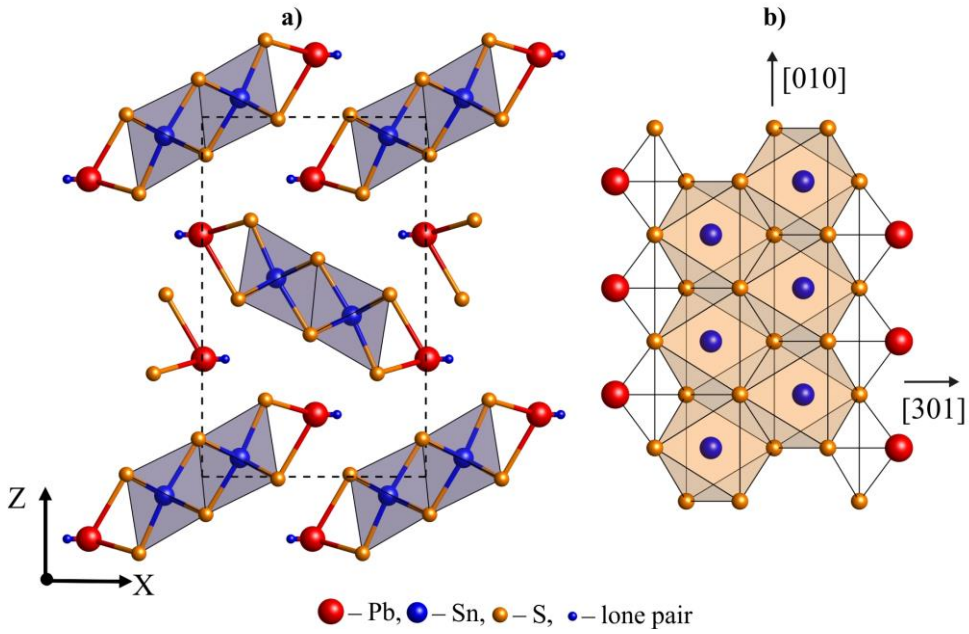

Fig. 1. $PbSnS_3$ crystal structure projection onto XZ plane (*a*) and isolated ribbon fragment extended in [010] direction (*b*).

Semiconductor Physics, Quantum Electronics & Optoelectronics, 2015. V. 18, N 1. P. 12-19.
doi: 10.15407/ spqeo18.01.012

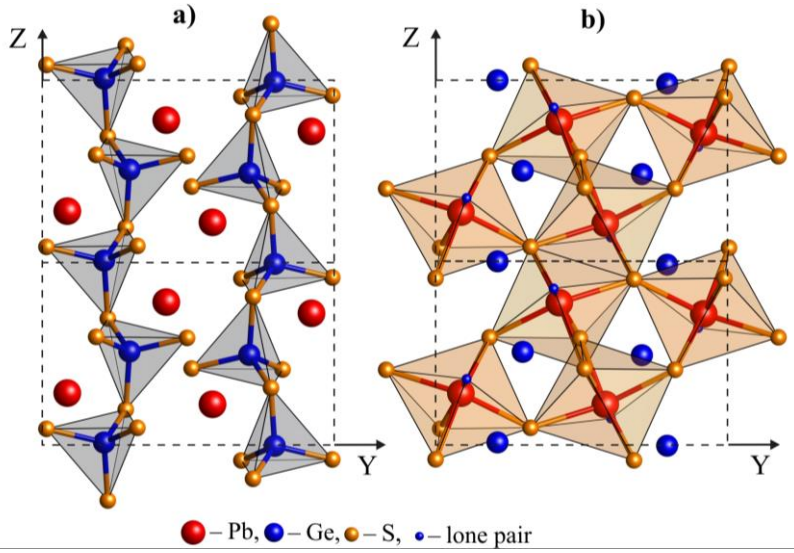

Fig. 2. $PbGeS_3$ crystal structure projection onto YZ plane with the distinguished chains of [GeS_4] tetrahedra (*a*) and [PbS_5•E•] ψ-octahedra (*b*).

Lead thiogermanate is formed due to the peritectic reaction at 866 K and crystallizes in the monoclinic structure with the lattice parameters a = 7.224 Å, b = 10.442 Å, c = 6.825 Å, β = 105.7°, Z = 4, space group $P2_1/c$ [14]. The unit cell of $PbGeS_3$ contains four bivalent lead (Pb^{2+}) atoms, four tetravalent germanium (Ge^{4+}) atoms and twelve sulfur atoms. Bivalent Pb^{II} and tetravalent Ge^{IV}, and also three sulfur S(1), S(2), S(3) atoms occupy five different 4*e* positions of $P2_1/c$ space group. Germanium atoms, being coordinated by four sulfur atoms, are located in the centers of slightly deformed [GeS_4] tetrahedra that are linked among themselves by the common vertices in the infinite chains $(GeS_3)_n^{2n-}$ extended along Z axis (Fig. 2a). The unit cell contains two non-equivalent chains of [GeS_4] tetrahedra.

Sulfur atoms form around lead atoms tetragonal-pyramidal coordination polyhedra, which, being complemented by the lone-electron pair of lead, are interpreted as coordination [PbS_5•E•] ψ-octahedra (Fig. 2b). Interatomic distances of Pb–S in ψ-octahedra are from 2.74 to 3.02 Å, where 2.74 Å distance is the nearest vertex to the host atom in the opposite side of lone-electron pair •E• in the octahedron. These [PbS_5•E•] ψ-octahedra are quite strongly distorted due to the absence of one of the ligands. The [PbS_5•E•] ψ-octahedra, being combined between themselves by common edges, form the zigzag chains extended along Z axis (Fig. 2b), which through the bridging sulfur atoms "sew" between themselves tetrahedral chains $(GeS_3)_n^{2n-}$, as a result, it leads to formation of goffered layer packages. Thus, $PbGeS_3$ crystals are chain-layered.

3. Calculation method

Energy band structure calculations were performed within the density functional theory (DFT) framework [15, 16] using the quantum-chemical software packages of ABINIT [17, 18] and SIESTA [19, 20]. The first package (ABINIT) uses the plane-wave (PW) basis, and the second package (SIESTA) – the linear combination of atomic orbitals (LCAO). The calculations procedure uses first-principal atomic normconserving pseudopotentials [21] of electronic configurations: for Ge atoms – [Ne] $3s^23p^4$, for Sn atoms – [Kr] $5s^25p^2$, for Pb atoms – [Xe] $5d^{10}6s^26p^2$, for S atoms – [Ne] $3s^23p^4$. The specified states belong to valence shells, [Ne], [Kr], [Xe] – to the core. Exchange-correlation interaction was considered in local density approximation (LDA) [22] and generalized gradient approximation (GGA) [23]. All the calculations were performed for the optimized structures without considering the spin-orbital interaction. The calculations by both packages provide the qualitatively and quantitatively similar results.

The density of states was calculated using the modified tetrahedron method. The electronic density was calculated using the method of special points. The nature of electronic states was analyzed using the partial density of states and the electronic density of isolated groups in the valence bands. The character of chemical bond was ascertained on the basis of valence electronic density calculations.

4. Results and discussion

4.1. Band structure and density of electronic states

Dispersion curves of $E(\boldsymbol{k})$ for the symmetric points and directions of the reciprocal space in the Brillouin zone for orthorhombic $PbSnS_3$ (Fig. 3a) and monoclinic $PbGeS_3$ (Fig. 3b) lattices are shown in Fig. 4a and 4b, respectively. The top of valence band is chosen as the origin of energy scale.

The important classification principles of electronic structure analysis of the valence band of crystals are as

Semiconductor Physics, Quantum Electronics & Optoelectronics, 2015. V. 18, N 1. P. 12-19.
doi: 10.15407/ spqeo18.01.012

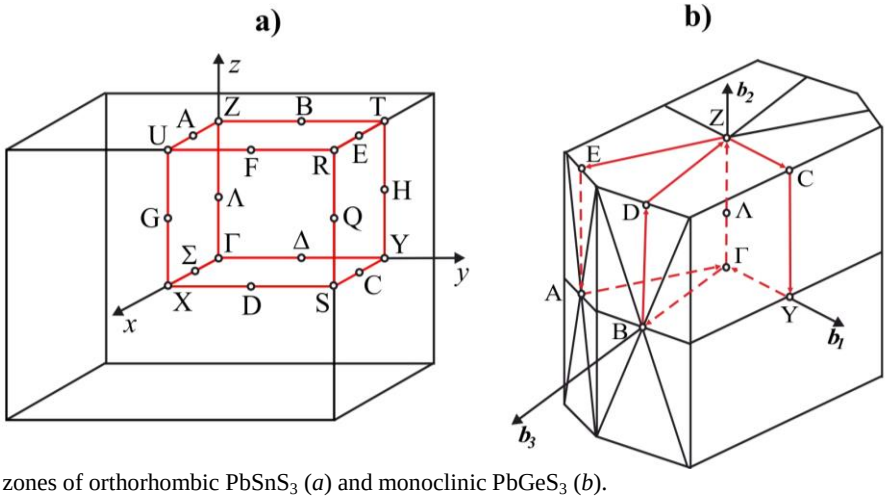

Fig. 3. Brillouin zones of orthorhombic $PbSnS_3$ (*a*) and monoclinic $PbGeS_3$ (*b*).

follows: the number of valence electrons that allows to determine the quantity of valence bands (dispersion branches), the type of partner in the chemical bond (it defines the relative energy location of the valence subbands), and the crystal structure of compound (it indicates the splitting of states, in particular the upper subbands in the valence band) [24]. The total number of valence electrons in $PbSnS_3$ and $PbGeS_3$ is identical and equal 144, hence, the energy spectrum $E(\boldsymbol{k})$ of the valence band consists of 72 dispersion branches grouped into four well energy-separated subbands. The valence subbands are numbered from the top as VBI, VBII, VBIII, and VBIV for the convenience of subsequent analysis of their nature formation.

It follows from $PbSnS_3$ and $PbGeS_3$ electronic structure calculations that both crystals are indirect-gap semiconductors with the calculated band-gaps E_{gi} = 0.75 eV (transition $\Sigma \rightarrow Z$) and E_{gi} = 1.96 eV (transition $Y \rightarrow \Gamma$), respectively. It was obtained the close calculated value of indirect gap E_{gi} = 0.71 eV for $PbSnS_3$ [12]. It should be noted that calculations from first-principles within the density functional theory with LDA as well as GGA approaches give the underestimated values of the band-gap widths for both crystals in comparison with the experimental data ($E_{gi}^{\exp}$ = 1.05 eV for $PbSnS_3$ [3] and $E_{gi}^{\exp}$ = 2.57 eV for $PbGeS_3$ [9, 10]), which is a systematic error of DFT methods. Despite this disadvantage, the local density approach is successfully used for the analysis of: *a*) trends in the changes of the total width of the valence band, the width and character of band-gap for the isoelectronic (cognate) crystals, *b*) the formation nature of occupied and unoccupied states, *c*) the spatial distribution of valence charge, *d*) the type of chemical bond.

The total valence band width in both compounds is initially defined by a relative location (arrangement) of *s*- and *p*-states of anions (S atoms), which is increased by cation contributions (*d*-states of Pb atoms and *s*-, *p*-states of Sn(Ge) atoms), and it is 16.45 eV for $PbSnS_3$ and 16.11 eV for $PbGeS_3$ in LDA approach. Hence, substitution of germanium atoms by the heavier tin ones is accompanied by changing cation coordinations and rising the crystal symmetry, which finally leads to insignificant increasing the total valence band width, and significant decreasing the band gap value.

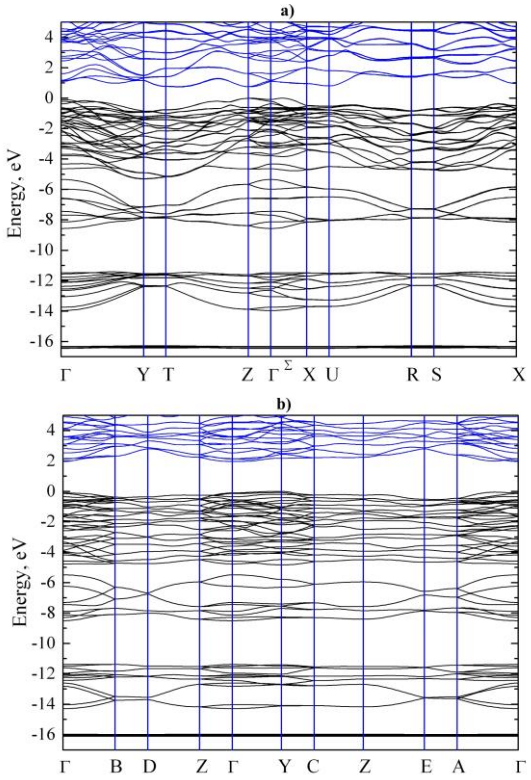

Fig. 4. Energy bands of $PbSnS_3$ (*a*) and $PbGeS_3$ (*b*) crystals corresponding to the occupied and unoccupied states calculated within the density functional method.

The calculations of the total and partial densities of states (Fig. 5) were made for clarification of the nature of crystal orbitals affiliating to the valence bands. The analysis of partial contributions into electronic density allows us to identify the genetic origin of valence subbands. From the analysis of energy distribution of local partial densities of states for lead, tin, germanium and sulfur it follows that *s*-, *p*- and *d*-states give different contributions to each of four occupied subbands and they differ by values. Non-equivalent atoms also give the different contributions to formation of energy bands. The *s*- and *p*-states of sulfur have the greatest statistical weight in $PbSnS_3$ and $PbGeS_3$ electronic structure. Despite the fact that *s*-band of sulfur contributes substantially to the distribution of density of valence electrons, *p*- and *s*-bands of sulfur can be considered as relatively independent at the analysis of energy spectrum and related density of energy states. For example, the total density of states for both compounds in the energy region from ~ –5 to 0 eV, i.e. in the upper valence subband (VBI), almost completely coincides with the partial density of *p*-states of sulfur, and VBIII subband is defined by *s*-states of sulfur. The inclusion of Pb*d*-orbitals in the system of basic functions has small effect on the valence band shape, but it leads to formation of the lowest quasi-core occupied subband (VBIV) (Figs. 5a and 5b). Its width does not exceed 0.2 eV, which indicates on a weak hybridization of Pb*d*-states with the states of other symmetry types.

In contrast to quasi-core Pb*d*-band, the structure of the following three valence subbands in both compounds is defined by the hybridization nature of *s*- and *p*-states of cations and anion. Moreover, each of these three following subbands can be conditionally separated into two parts formed by the different states. Thus, the third valence subband (VBIII) is mainly formed by S3*s*-states with a small admixture of Sn5*s*-(Ge4*s*-) states in its lower part and Sn5*p*-, 5*d*- (Ge4*p*-, 4*d*-) states in its upper part.

The second bunch of eight valence branches (VBII) is formed by 3*p*-states of sulfur and *s*-states of lead and tin (germanium), the contribution of Pb6*s*-states of lone pair prevails in the lower part of this band, and Sn5*s*-(Ge4*s*-) states in its upper part. The uppermost valence subband (VBI) also consists of two parts: the bottom, it is constructed by 3*p*-orbitals of sulfur and Sn5*p*- (Ge4*p*-) states; the top, it is mainly formed by S3*p*-states with an insignificant admixture of Sn5*d*- (Ge4*d*-) states and Pb6s-, 6*p*-states. In general, the whole region of valence states in the energy range from 0 to –14 eV has the complex hybrid character caused by the interaction of all types of atoms inherent to this compound.

The conduction band, as well as the valence band, has a mixed character for the structure of atomic states, and it is formed by free *p*-states of sulfur, *s*-, *p*-states of tin (germanium) and *p*-states of lead. In $PbGeS_3$, also *d*-states of sulfur and germanium are admixed to these states. Hence, the electronic states near the bottom of the conduction band have mixed anion-cation nature in both crystals.

Thus, the structures of the occupied and unoccupied energy bands (the quantity of subbands, their sequence, the relative composition, the nature of their constituent states) are largely similar for $PbSnS_3$ and $PbGeS_3$ crystals. Moreover, 6*s*-states of lone-electron

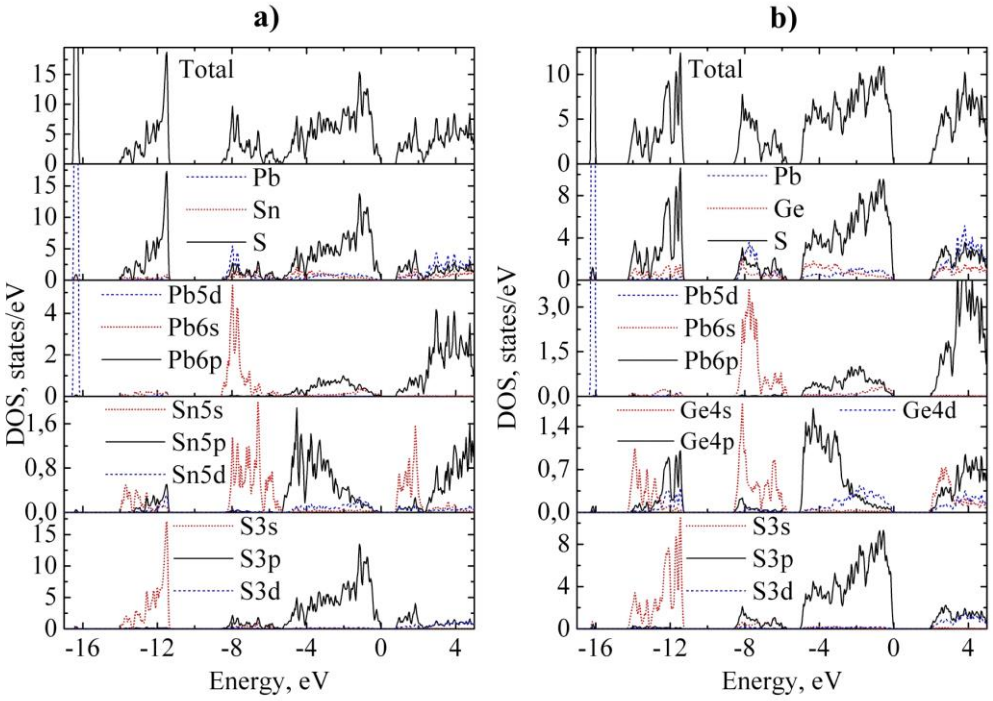

Fig. 5. Total and partial densities of states of $PbSnS_3$ (*a*) and $PbGeS_3$ (*b*).

pair of lead in both crystals make the significant contribution to formation of the middle occupied subband (VBII) and the insignificant contribution to the uppermost part of valence band formed mainly by 3*p*-orbitals of sulfur atoms.

4.2. The spatial distribution of valence charge

Material properties are defined by the spatial and energy electronic structures. Thus, the particular interest represents the electronic structure of valence electrons, which characteristically changes at an appearance of the chemical bond between atoms. It is necessary to know the overall picture of the spatial electronic density distribution for the exact description of the chemical bond. However, it is very difficult to obtain this information by using X-ray and neutron scattering experimental methods for these complexes by their structure $PbSnS_3$ and $PbGeS_3$ crystalline materials. It is much easier and convenient to perform the theoretical calculations of electronic density distribution. The calculated electronic density allows us to build the maps of spatial electronic density distribution of $PbSnS_3$ and $PbGeS_3$ cells and compare the distribution nature in different crystallographic planes.

Since the lone-electron pair of bivalent lead (Pb^{II}) participates in formation of crystal and electronic structures of $PbSnS_3$ and $PbGeS_3$, it is very important to visualize it, which is possible if performing 3D-representation for the spatial distribution of the total electronic density (Fig. 6). From this figure, it is clear that the electronic density distribution increases along Pb–S bonds as well as at the periphery of lead atoms in [PbS_3•E•] ψ-tetrahedra of $PbSnS_3$ crystal and [PbS_5•E•] ψ-octahedra of $PbGeS_3$ crystal. The latter information is in accordance with the notion for the lone pairs of electrons localized in certain space sectors surrounding these atoms. Symbol •E• in Fig. 6 designates the part of the electron charge of the lone pair near lead atoms. If we draw the vector connecting the nucleus of lead atom with the center of the highest density area of the lone pair, it is possible to verify that it is directed toward the depth of van der Waals space.

The isosurfaces ρ(***r***) in [PbS_5•E•], [SnS_6] octahedra and [PbS_3•E•], [GeS_4] tetrahedra are strongly deformed along Pb–S, Sn–S, Ge–S bond directions. The distribution shape of isosurface ρ(***r***) in $PbSnS_3$ (Fig. 6, *a*) shows formation of strong interatomic interactions between cations and anions inside isolated ribbons and the presence of weak van der Waals interaction between anions belonging to the neighbor ribbons with participation of the lone pair of Pb^{II} atoms.

The contour maps for the constant electronic density ρ(***r***) give additional information about valence charge distribution in $PbSnS_3$ and $PbGeS_3$ crystals. Fig. 7a shows the map for the electronic density distribution in $PbSnS_3$ crystal within the plane intersecting one isolated ribbon along Sn–S, Pb–S bonds in double [$Sn^{IV}S_6$] octahedra and [$Pb^{II}S_3$•E•] ψ-tetrahedra adjacent to them. High concentrations of electrons near localization places of S, Sn, Pb atoms are inherent to the contribution contours of core electrons. From Fig. 7a it is clear that the electronic density concentrates mainly in [$Sn^{IV}S_6$] octahedra and [$Pb^{II}S_3$•E•] ψ-tetrahedra, which form the endless ribbons. Localized maxima of electronic density on cation-anion bonds are connected among themselves by

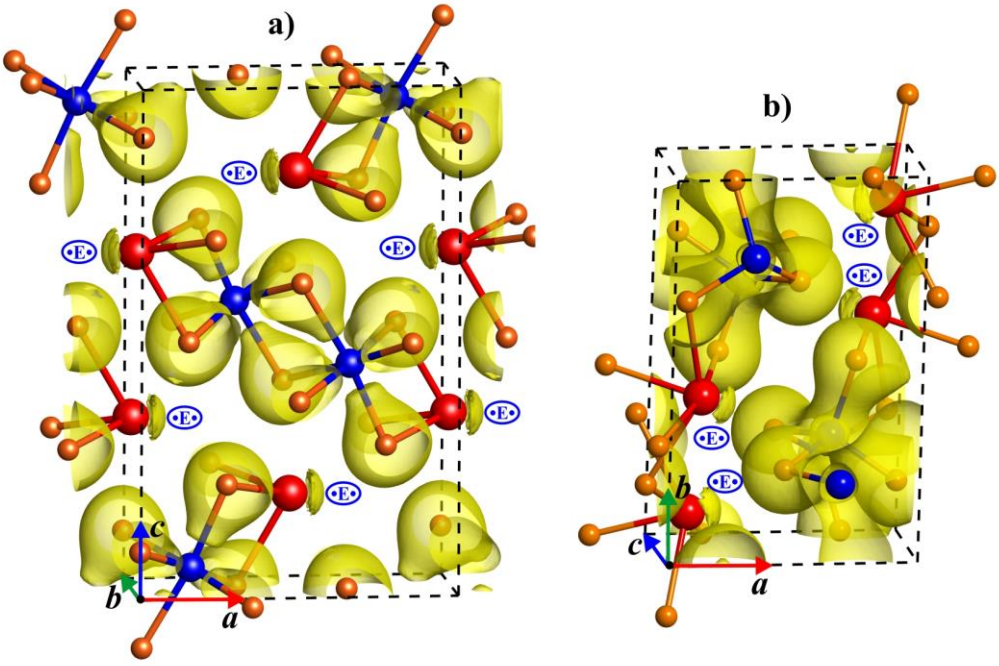

Fig. 6. 3D-images of spatial electronic density distribution of $PbSnS_3$ (*a*) and $PbGeS_3$ (*b*) crystals.

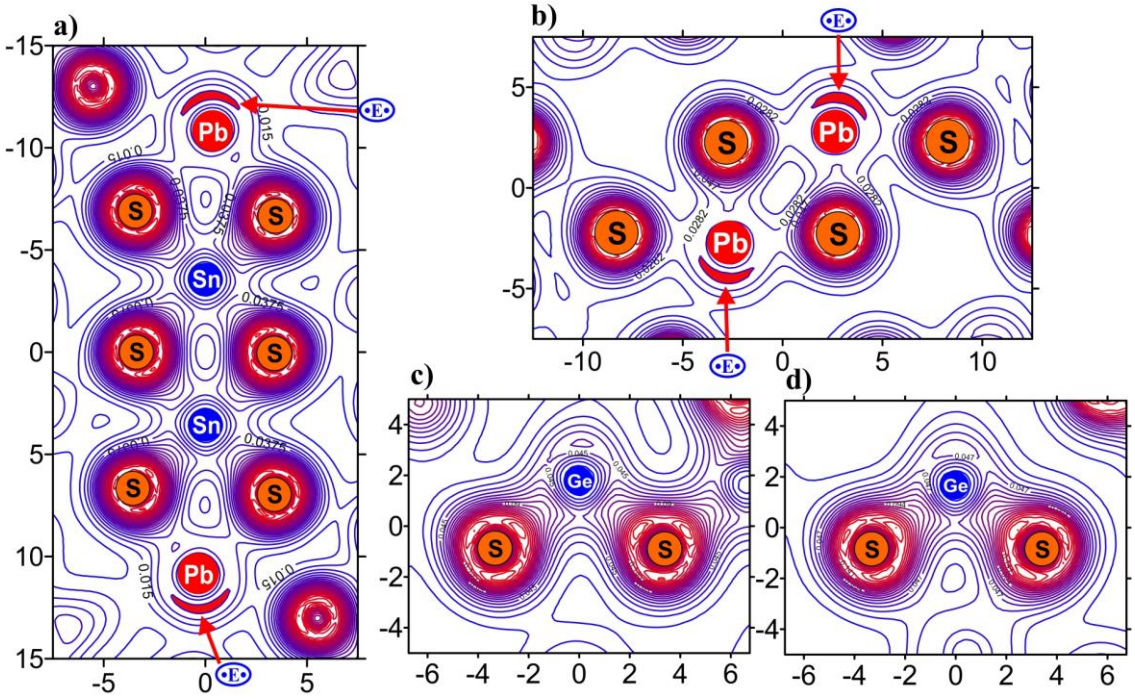

Fig. 7. Spatial distribution maps of electronic density for $PbSnS_3$ (*a*) and $PbGeS_3$ (*b–d*) crystals built in different planes: along bonds in ribbon (*a*), along common edge of doubled [PbS_5•E•] ψ-octahedra (*b*), and along common vertices of [GeS_4] tetrahedron in the direction of S–Ge–S chains (*c*) and perpendicular to these chains (*d*).

the common contours of constant charge density and characterize the covalent component of chemical bonds. The presence of covalent component of bond in $PbSnS_3$ is caused by hybridization of S3*p*-states with Pb6*p*-, Sn5*p*-states (Fig. 5a), which are responsible for the stability of octahedral-tetrahedral structure of this compound. The ionic bond is characterized by the charge increasing around anions and the charge decreasing on covalent bonds between ions.

For the $PbGeS_3$ case, the choice of suitable planes for contour maps is limited by the complexity of crystal structure in this compound. In this case, the most suitable planes are the planes through four sulfur atoms and two lead atoms of edge-doubled [PbS_5•E•] octahedra (Fig. 7b) and through two sulfur atoms and one germanium atom of [GeS_4] tetrahedron (Fig. 7c and 7d). Germanium and sulfur atoms are united (combined) by the overall contour electronic density lines, thus forming the [GeS_4] molecular structural unit. It is obvious from Fig. 7b that the asymmetric distribution of valence charge around Pb atom with some maximum corresponds to the position of a lone pair. Figs. 7c and 7d also show a stronger interaction between Ge and S atoms belonging to [GeS_4] tetrahedron compared to Pb–S bond inside [PbS_5•E•] octahedron.

5. Conclusions

The calculations of band structure, total and partial densities of states, the distribution of valence electron density of $PbSnS_3$ and $PbGeS_3$ ternary compounds with mixed cation coordination have been performed within the unified framework of density functional theory method. It has been found that the structures of occupied and unoccupied energy bands (the subband quantity, their sequence, the relative composition, the nature of their constituent states, and the character of dispersion dependence) of these compounds are largely similar among themselves. Both crystals are indirect-gap semiconductors, which band-gap width essentially decreases after substitution of germanium atoms with the heavier tin ones.

Visualization of the lone-electron pair of bivalent lead is implemented using 3D-representation of spatial distribution of the total electronic density. It is identified participation of Pb6*s*-states of lone pairs in formation of the second occupied subband and the top of valence band, which is also the common feature of electronic spectra inherent to these compounds. The electron charge distribution characterizes $PbSnS_3$ and $PbGeS_3$ crystals as the covalent-ion one with the prevailing charge concentration on Ge–S, Sn–S, Pb–S bonds, which are formed in accord with the donor-acceptor mechanism.

References

1. D.I. Bletskan, *Crystalline and Glassy Chalcogenides of Si, Ge, Sn and Alloys on Their Base*. Vol. 1. Zakarpattia, Uzhhorod, 2004.

2. W.H. Paar, R. Miletich, D. Topa, A.J. Criddle, M.K. De Brodtkorb, G. Amthauer, G. Tippelt, Suredaite, $PbSnS_3$, a new mineral species, from Pirquitas Ag–Sn deposit, NW-Argentina: mineralogy and crystal structure // *Amer. Miner.*, **85**, p. 1066-1075 (2000).
3. U.V. Alpen, J. Fenner, E. Gmelin, Semiconductors of the type $Me^{II}Me^{IV}S_3$ // *Mater. Res. Bull.*, **10**(3), p. 175-180 (1975).
4. T.A. Kuku, S.O. Azi, O. Osasona, Electrical properties of vacuum evaporated $PbSnS_3$ thin films // *J. Mater. Sci.* **41**(4), p. 1067-1071 (2006).
5. T.A. Kuku, S.O. Azi, Optical properties of evaporated $PbSnS_3$ thin films // *J. Mater. Sci.* **33**(12), p. 3193-3196 (1998).
6. D.I. Bletskan, V.M. Kabatsii, T.A. Sakal, V.A. Stefanovych, Structure and vibrational spectra of $M^{II}A^{IV}B_{3VI}$-type crystalline and glassy semiconductors // *J. Non-Cryst. Solids*, **326-327**, p. 77-82 (2003).
7. Z.V. Popovič, Infrared and Raman spectra of $PbGeS_3$ // *Physica B*, **119**(3), p. 283-289 (1983).
8. Z.V. Popovič, The vibrational properties of $PbGeS_3$ single crystal // *Fizika Tverd. Tela*, **28**(2), p. 344-351 (1986).
9. D.I. Bletskan, V.M. Kabatsii, I.P. Studenyak, V.V. Frolova, Edge absorption spectra of crystalline and glassy $PbGeS_3$ // *Optics and Spectroscopy*, **103**(5), p. 772-776 (2007).
10. D.I. Bletskan, V.M. Kabatsii, Photoelectric properties of crystalline and glassy $PbGeS_3$ // *Open J. Inorg. Non-Met. Mater.* **3**(3), p. 29-36 (2013).
11. M.M. Bletskan, Electronic structure of $PbSnS_3$ // *VI Intern. conf. on Actual problems of Solid State Physics "FTT–2013"*, Minsk, Belarus, **2**, p. 82-84 (2013).
12. N.N. Omehe, S. Eshika, S.O. Azi, Electronic and vibrational properties of $PbSnS_3$ // *IOSR J. Electr. Electr. Eng.*, **5(**5), p. 12-17 (2013).
13. J.C. Jumas, M. Ribes, E. Philippot, M. Maurin, Sur le systeme SnS_2–PbS. Structure crystalline de $PbSnS_3$ // *C.R. Acad. Sci. C* (*Paris*), **275**, p. 269-272 (1972).
14. M. Ribes, J. Qlivier-Fourcade, E. Philippot, M. Maurin, Structure Cristalline d'un Tiogermanate de Plomb a Chaines Infinies $(PbGeS_3)_n$ // *Acta Crystallogr. B*, **30(**6), p. 1391-1395 (1974).
15. P. Hohenberg, W. Kohn, Inhomogeneous electron gas // *Phys. Rev.* **136(**3), p. B864-B871 (1964).
16. W. Kohn, L.J. Sham, Self-consistent equations including exchange and correlation effects // *Phys. Rev.* **140(**4), p. A1133-A1138 (1965).
17. X. Gonze, J.-M. Beuken, R. Caracas et al., First-principle computation of material properties: the ABINIT software project // *Comp. Mat. Sci. B*, **25**(3), p. 478-492 (2002).
18. http://www.abinit.org/
19. J.M. Soler, E. Artacho, J.D. Gale, A. Garcia, J. Junquera, P. Ordejon, D. Sanchez-Portal, The SIESTA method for ab initio order-N materials simulation // *J. Phys.: Condens. Matter*, **14**(11), p. 2745-2779 (2002).
20. http://departments.icmab.es/leem/siesta/
21. C. Hartwigsen, S. Goedecker, J. Hutter, Relativistic separable dual-space Gaussian pseudopotentials from H to Rn // *Phys. Rev. B*, **58**(7), p. 3641-3662 (1998).
22. D.M. Ceperley, B.J. Alder, Ground state of the electron gas by a stochastic method // *Phys. Rev. Lett.* **45(**7), p. 566-569 (1980).
23. J.P. Perdew, J.A. Chevary, S.H. Vosko, K.A. Jackson, M.R. Pederson, D.J. Singh, C. Fiolhais, Atoms, molecules, solids, and surfaces: Applications of the generalized gradient approximation for exchange and correlation // *Phys. Rev. B*, **46**(11), p. 6671-6687 (1992).
24. A. Meisel, G. Leonhardt, R. Szargan, *Röntgenspektren und Chemische Bindung*. Akademische Verlagsgesellschaft Geest & Portig K.-G., Leipzig, 1977.